

# Thermodynamic Stability of Water Molecules in the Bacteriorhodopsin Proton Channel: A Molecular Dynamics Free Energy Perturbation Study

Benoît Roux,\* Mafalda Nina,<sup>#</sup> Régis Pomès,\* and Jeremy C. Smith<sup>#</sup>

\*Groupe de Recherche en Transport Membranaire (GRTM), Départements de physique et chimie, Université de Montréal, Montréal, Québec, Canada H3C 3J7; and <sup>#</sup>Section de Biophysique des Protéines et des Membranes, Département de Biologie Cellulaire et Moléculaire, CEA-Saclay, 91191 Gif-sur-Yvette, France

**ABSTRACT** The proton transfer activity of the light-driven proton pump, bacteriorhodopsin (bR) in the photochemical cycle might imply internal water molecules. The free energy of inserting water molecules in specific sites along the bR transmembrane channel has been calculated using molecular dynamics simulations based on a microscopic model. The existence of internal hydration is related to the free energy change on transfer of a water molecule from bulk solvent into a specific binding site. Thermodynamic integration and perturbation methods were used to calculate free energies of hydration for each hydrated model from molecular dynamics simulations of the creation of water molecules into specific protein-binding sites. A rigorous statistical mechanical formulation allowing the calculation of the free energy of transfer of water molecules from the bulk to a protein cavity is used to estimate the probabilities of occupancy in the putative bR proton channel. The channel contains a region lined primarily by nonpolar side-chains. Nevertheless, the results indicate that the transfer of four water molecules from bulk water to this apparently hydrophobic region is thermodynamically permitted. The column forms a continuous hydrogen-bonded chain over 12 Å between a proton donor, Asp 96, and the retinal Schiff base acceptor. The presence of two water molecules in direct hydrogen-bonding association with the Schiff base is found to be strongly favorable thermodynamically. The implications of these results for the mechanism of proton transfer in bR are discussed.

## INTRODUCTION

Bacteriorhodopsin (bR) is a light-driven proton pump found in the purple membrane of the bacterium *Halobacterium halobium* (Oesterhelt et al., 1971, 1973). The experimental structure of bR determined at atomic resolution from cryo-electron microscopy revealed a channel containing the Schiff base of the retinal chromophore (Henderson et al., 1990). Site-directed mutagenesis and vibrational spectroscopy experiments have enabled the identification of polar residues in the channel involved in the proton transfer pathway (Mogi et al., 1987, 1988; Stern and Khorana, 1989; Marti et al., 1991). Several lines of evidence indicate that water molecules may also be present in the channel and may play an important functional role. Although the cryoelectron microscopy structure lacks sufficient resolution to locate water molecules, a contrast variation neutron diffraction study has indicated that there are approximately four water molecules present in the neighborhood of the Schiff base (Papadopoulos et al., 1990). Spectroscopic experiments suggest that one or more water molecules are directly hydrogen bonded to the Schiff base (Hildebrandt and Stockburger, 1984; Harbison et al., 1988; De Groot et al., 1990; Deng et al., 1994; Fischer et al., 1994).

In previous papers, *ab initio* quantum chemical calculations were performed on Schiff base-water complexes to investigate possible direct hydrogen-bonding interactions

(Nina et al., 1993, 1995). Two minimal-energy interaction sites were found; one involves a hydrogen bond with the Schiff base NH group, which in light-adapted bR is in a polar environment on the extracellular side of the Schiff base, and the other involves a CH $\cdots$ O hydrogen bond on the cytoplasmic side (see Fig. 1). Other water molecules, not directly associated with the Schiff base, may also be involved in the proton transfer pathway. The reprotonation step at the end of the photocycle involves the transfer of a proton from Asp 96, a residue near the cytoplasmic surface, to the retinal Schiff base (Otto et al., 1989; Holz et al., 1989; Butt et al., 1989; Gerwert et al., 1989). This requires the translocation of a proton over a distance of 10 to 12 Å through a narrow region of the channel lined with nonpolar residues. The question arises as to how the proton is transferred across this region. One possibility is that a number of water molecules could form a proton transfer chain from Asp 96 to the Schiff base (Cao et al., 1991). Although the chain of water molecules could be stabilized by making hydrogen bonds to each other, and perhaps to Thr 46 and Thr 89 (Rothschild et al., 1992), preliminary analysis of the bR structure suggests that it would be primarily located in a nonpolar cavity. More generally, water molecules in buried protein cavities can play an important functional role (Edsall and McKenzie, 1983; Meyer, 1992; Williams et al., 1994). This raises important questions concerning the thermodynamic stability of water molecules in such an environment.

The goal of the present paper is to investigate the thermodynamic stability of water molecules in the bR proton channel using molecular dynamics simulations and free energy calculations. Whether a given protein cavity should

Received for publication 21 March 1996 and in final form 16 April 1996.

Address reprint requests to Dr. Benoît Roux, Chemistry Department, Université de Montréal, C. P. 6128, Succ. A, Montréal H3C 3J7, Canada. Tel.: 514-343-7105; Fax: 514-343-7586; E-mail: rouxb@ere.umontreal.ca.

© 1996 by the Biophysical Society

0006-3495/96/08/670/12 \$2.00

be occupied by water molecules depends on the environment it provides. A qualitative appreciation of water occupancy can sometimes be gained by examining the size and shape of the cavity and the hydrophobic or hydrophilic nature of the side-chains lining it. However, a more rigorous analysis requires the determination of thermodynamic quantities, in particular, the free energy of transfer of a water molecule from bulk solvent to the buried site considered. A theoretical determination of this quantity is therefore of basic interest in understanding cavity hydration. Moreover, theoretical analysis may be of use in analyzing the likelihood of occupancy of sites not amenable to experimental determination. For example, this problem can arise in crystallographic analyses of water molecules with partial occupancies and/or high thermal fluctuations or at a resolution insufficient for their characterization. To investigate the thermodynamic stability and probability of occupancy of water molecules in specific sites in the channel of bR we used molecular dynamics free energy perturbation methods.

In principle, the free energy of transfer can be determined using molecular dynamics simulations. However, as residence times of buried water molecules can be on the nanosecond to microsecond time scale, indicating the presence of significant energy barriers to their migration (Desinov et al., 1995), water molecules are not expected to partition into the interior of proteins according to thermodynamic equilibrium in standard picosecond time scale molecular dynamics calculations (Brooks et al., 1988). Consequently, specialized molecular dynamics techniques must be employed. To this end, Wade et al. (1990, 1991) have used thermodynamic perturbation theory combined with molecular dynamics to calculate the free energy of inserting water molecules inside a sulfate-binding protein. The values obtained are consistent with crystallographic observation. But practical and theoretical problems remain in such calculations. In particular, the perturbation was calculated relative to a free unbound reference state (Wade et al., 1990, 1991). It follows that the position of the inserted water molecule is not restricted to the cavity when it is weakly coupled to its surroundings near the end-point of the thermodynamic integration and it can diffuse away during the free energy simulation. A treatment by Hermans and co-workers (Hermans and Shankar, 1986; Chang and Hermans, submitted) avoids this problem by applying a harmonic restraining potential to the inserted particle in the non-interacting reference state. However, there is no unique choice for the value of the force constant used in the restraining potential, and the significance of the calculated free energy is unclear. Thus, although the previous methods for calculating the thermodynamic stability of water molecules in protein cavities provided elements essential for solving the problem, some fundamental theoretical aspects need consideration.

In the first part of this paper we address these problems and the previous approaches (Hermans and Shankar, 1986; Wade et al., 1990, 1991; Chang and Hermans, submitted) are extended to allow a rigorous discussion of the thermodynamic stability of water molecules inside the bR proton

channel. In particular, mathematical expressions suitable for evaluation from computer simulations are derived for the binding constant and the probability of finding any number of water molecules in isolated cavities. The binding free energy contribution of the restraining potential applied in the reference state is treated analytically and its significance is clarified. The present formalism is general and can be applied to investigate the binding constant and the probability of occupancy of any molecule in a specific site in a macromolecule. In the second part of the paper, hydrated models of bR are constructed and the computational details are described. In particular, the probability of water occupancy is calculated using free energy molecular dynamics simulations. The calculations provide a quantitative basis for the thermodynamic description of functionally important internal water molecules in bR. The results suggest that the transfer of four water molecules from bulk water to bR, so as to form an intact hydrogen-bonded column between the proton donor, Asp 96, and the Schiff base, is thermodynamically permitted. Moreover, it is found that the presence of each of two water molecules directly hydrogen bonded to the Schiff base is strongly favored thermodynamically. The functional significance of these results is discussed. The paper is concluded with a perspective on future experiments.

## MATERIALS AND METHODS

### Free energy and probability of water occupancy

We consider an isolated cavity located inside a protein in thermodynamic equilibrium with a large number,  $N$ , of bulk water molecules. The system is such that two distinct regions in space, the cavity and the bulk regions, can be distinguished. This implies that any volume integral can be expressed as the sum of the integrals over the two separate regions:

$$\int d\mathbf{r} \cdots \equiv \int_{\text{cavity}} d\mathbf{r} \cdots + \int_{\text{bulk}} d\mathbf{r} \cdots \quad (1)$$

Thus, for any instantaneous configuration of the water-protein system, the total number of water molecules inside the cavity can be represented by the discrete function  $n'(r_1, r_2, \dots, r_n)$ , defined as

$$n'(r_1, r_2, \dots, r_n) = \int_{\text{cavity}} d\mathbf{r} \sum_i \delta(\mathbf{r} - \mathbf{r}_i), \quad (2)$$

where  $r_i$  is the position of the oxygen of the  $i$ th water molecule and the subscript of the integral sign implies that the integral is taken over the volume of the cavity. The probability,  $P_n$ , of having exactly  $n$  water molecules inside the cavity is calculated from the average:

$$P_n = \langle \delta_{nn'} \rangle, \quad (3)$$

where  $\delta_{nn'}$  is a Kronecker discrete delta function:

$$\delta_{nn'} = \begin{cases} 1 & \text{if } n = n'(r_1, r_2, \dots, r_n) \\ 0 & \text{otherwise.} \end{cases} \quad (4)$$

The completeness of the Kronecker delta,  $\sum_n \delta_{nn'} = 1$ , ensures that  $P_n$  is normalized, i.e.,  $\sum_n P_n = 1$ .

To derive expressions for the occupancy probabilities that can be evaluated from computer simulations, it is useful to consider the probability ratio  $R_n = P_n/P_{n-1}$ .  $R_n$  is proportional to the reversible thermodynamic work needed to remove one water molecule from the bulk solution and

insert it into the cavity, given that the cavity already contains  $n - 1$  waters (see below). For  $n = 1$ , this is given by

$$R_1 = \frac{\int d(1) \cdots \int d(N) \int d\Gamma \delta_{1,n'} e^{-U/k_B T}}{\int d(1) \cdots \int d(N) \int d\Gamma \delta_{0,n'} e^{-U/k_B T}}, \quad (5)$$

where  $U$  is the total potential energy of the system and  $(1, 2, \dots, N)$  and  $\Gamma$  are the degrees of freedom of the water molecules and the protein atoms, respectively. As the factor  $\delta_{1,n'}$  in the integrand is zero unless one of the  $N$  water molecules is located inside the cavity,  $R_1$  may be rewritten as,

$$R_1 = N \frac{\int_{\text{cavity}} d(1) \int_{\text{bulk}} d(2) \cdots \int_{\text{bulk}} d(N) \int d\Gamma e^{-U/k_B T}}{\int_{\text{bulk}} d(1) \int_{\text{bulk}} d(2) \cdots \int_{\text{bulk}} d(N) \int d\Gamma e^{-U/k_B T}}, \quad (6)$$

where water molecule number 1 is chosen arbitrarily to occupy the cavity. The factor  $N$  is included to account for the multiple ways to obtain equivalent configurations. More generally,  $R_n$  is

$$R_n = \frac{N!/(n!(N-n)!)}{N!/((n-1)!(N-n+1)!)} \times \quad (7)$$

$$\frac{\int_{\text{cavity}} d(1) \cdots \int_{\text{cavity}} d(n) \int_{\text{bulk}} d(n+1) \cdots \int_{\text{bulk}} d(N) \int d\Gamma e^{-U/k_B T}}{\int_{\text{cavity}} d(1) \cdots \int_{\text{cavity}} d(n-1) \int_{\text{bulk}} d(n) \cdots \int_{\text{bulk}} d(N) \int d\Gamma e^{-U/k_B T}},$$

as there are  $N!/(n!(N-n)!)$  equivalent configurations with exactly  $n$  water molecules in the cavity. In the thermodynamic limit,  $N \rightarrow \infty$  and the prefactor  $(N-n)/n \approx N/n$ .

To make further progress in obtaining an expression that can be evaluated through a computer simulation, it is useful to define  $U_1$  as the total potential energy of the fully interacting system and  $U_0$  as the total potential energy of a fictitious system in which water molecule number 1 is invisible and does not interact with its surroundings. Rewriting Eq. 6 as

$$R_1 = N \frac{R_1^{\text{cavity}}}{R_1^{\text{bulk}}}, \quad (8)$$

we introduce  $U_1$  and  $U_0$  as follows:

$$R_1^{\text{cavity}} \quad (9)$$

$$= \left[ \frac{\int_{\text{cavity}} d(1) \int_{\text{bulk}} d(2) \cdots \int_{\text{bulk}} d(N) \int d\Gamma e^{-U_1/k_B T}}{\int d(1) \delta(r_1 - r^*) \int_{\text{bulk}} d(2) \cdots \int_{\text{bulk}} d(N) \int d\Gamma e^{-U_0/k_B T}} \right]$$

and

$$R_1^{\text{bulk}} \quad (10)$$

$$= \left[ \frac{\int_{\text{bulk}} d(1) \int_{\text{bulk}} d(2) \cdots \int_{\text{bulk}} d(N) \int d\Gamma e^{-U_1/k_B T}}{\int d(1) \delta(r_1 - r^*) \int_{\text{bulk}} d(2) \cdots \int_{\text{bulk}} d(N) \int d\Gamma e^{-U_0/k_B T}} \right].$$

As water molecule number 1 is non-interacting in the  $U_0$  fictitious system, the position  $r^*$  can be chosen arbitrarily in Eqs. 9 and 10. The term  $R_1^{\text{bulk}}$  may then be expressed as

$$\begin{aligned} R_1^{\text{bulk}} &= \int_{\text{bulk}} d\mathbf{r} \left[ \frac{\int_{\text{bulk}} d(1) \delta(r_1 - r) \int_{\text{bulk}} d(2) \cdots \int_{\text{bulk}} d(N) \int d\Gamma e^{-U_1/k_B T}}{\int d(1) \delta(r_1 - r^*) \int_{\text{bulk}} d(2) \cdots \int_{\text{bulk}} d(N) \int d\Gamma e^{-U_0/k_B T}} \right] \\ &= \int_{\text{bulk}} d\mathbf{r} e^{-\Delta A_{\text{bulk}}^{0 \rightarrow 1}/k_B T} \\ &= V_{\text{bulk}} e^{-\Delta A_{\text{bulk}}^{0 \rightarrow 1}/k_B T}, \end{aligned} \quad (11)$$

where  $\Delta A_{\text{bulk}}^{0 \rightarrow 1}$  corresponds to the free energy difference between a first system,  $U_1$ , in which the water molecule number 1 is fixed at an arbitrary point  $r$  in the bulk region and interacts with its surroundings and a second system,  $U_0$ , in which water molecule number 1 is invisible and fixed at an arbitrary point  $r^*$ . Because the free energy  $\Delta A_{\text{bulk}}^{0 \rightarrow 1}$  does not depend on  $r$ , by translational invariance of the bulk region, the volume integral simply results in a factor of  $V_{\text{bulk}}$  in Eq. 11. Similarly, the term  $R_1^{\text{cavity}}$  may be expressed as

$$\begin{aligned} R_1^{\text{cavity}} &= \int_{\text{cavity}} d\mathbf{r} \left[ \frac{\int_{\text{cavity}} d(1) \delta(r_1 - r) \int_{\text{bulk}} d(2) \cdots \int_{\text{bulk}} d(N) \int d\Gamma e^{-U_1/k_B T}}{\int d(1) \delta(r_1 - r^*) \int_{\text{bulk}} d(2) \cdots \int_{\text{bulk}} d(N) \int d\Gamma e^{-U_0/k_B T}} \right] \\ &= \int_{\text{cavity}} d\mathbf{r} e^{-W_{\text{cavity}}^{0 \rightarrow 1}(r)/k_B T}, \end{aligned} \quad (12)$$

where  $W_{\text{cavity}}^{0 \rightarrow 1}(r)$  is the potential of mean force (PMF) corresponding to the  $r$ -dependent free energy required to insert a water molecule at position  $r$  inside the cavity. As expressed in Eq. 12, the evaluation of  $R_1^{\text{cavity}}$  requires repeated calculations of the  $r$ -dependent function  $W_{\text{cavity}}^{0 \rightarrow 1}(r)$ , at a large number of positions, due to the explicit three-dimensional volume integration over  $r$ . In principle, this could be done by performing a large number of independent free energy simulations, fixing the water molecule at different points  $r$ . However, this would be computationally prohibitive. A more efficient method for evaluating Eq. 9 is thus desirable. Moreover, as the water molecule is not coupled to its surroundings in the  $U_0$  system, it is likely to leave the cavity near the end-point of the thermodynamic integration during a straight molecular dynamics trajectory, leading to errors. Therefore, an important methodological problem is the design of an effective computational approach to insert a water molecule in a cavity without biasing the results with restraining forces while ensuring an accurate sampling of the cavity volume at all points in the thermodynamic integration. This can be achieved using the following theoretical analysis. Eq. 9 can be rewritten including the harmonic potential,  $u(r_1) = \frac{1}{2} k_{\text{harm}}(r_1 - r^*)^2$ , acting only on the non-interacting invisible water molecule:

$$\begin{aligned} R_1^{\text{cavity}} &= \left[ \frac{\int_{\text{cavity}} d(1) \int_{\text{bulk}} d(2) \cdots \int_{\text{bulk}} d(N) \int d\Gamma e^{-U_1/k_B T}}{\int d(1) \int_{\text{bulk}} d(2) \cdots \int_{\text{bulk}} d(N) \int d\Gamma e^{-[U_0 + u(r_1)]/k_B T}} \right] \\ &\times \left[ \frac{\int d(1) \int_{\text{bulk}} d(2) \cdots \int_{\text{bulk}} d(N) \cdots \int d\Gamma e^{-[U_0 + u(r_1)]/k_B T}}{\int d(1) \delta(r_1 - r^*) \int_{\text{bulk}} d(2) \cdots \int_{\text{bulk}} d(N) \int d\Gamma e^{-U_0/k_B T}} \right] \\ &= e^{-\Delta A_{\text{cavity}}^{0 \rightarrow 1}/k_B T} \\ &\times \left[ \left( \frac{\int d(1) e^{-u(r_1)/k_B T}}{\int d(1) \delta(r_1 - r^*)} \right) \left( \frac{\int_{\text{bulk}} d(2) \cdots \int_{\text{bulk}} d(N) \int d\Gamma e^{-U_0/k_B T}}{\int_{\text{bulk}} d(2) \cdots \int_{\text{bulk}} d(N) \int d\Gamma e^{-U_0/k_B T}} \right) \right] \\ &= e^{-\Delta A_{\text{cavity}}^{0 \rightarrow 1}/k_B T} \left( \frac{2\pi k_B T}{k_{\text{harm}}} \right)^{3/2}, \end{aligned} \quad (13)$$

where  $\Delta A_{\text{cavity}}^{0 \rightarrow 1}$  corresponds to the free energy difference between a system of potential energy  $U_1$ , in which the interacting water molecule is free to move inside the cavity, and a system of potential energy  $U_0 + u(r_1)$ , in which the same water molecule is non-interacting but has its oxygen harmonically restrained around the point  $r^*$  with a force constant  $k_{\text{harm}}$ . The factor  $R_1$  is then

$$R_1 = \rho_{\text{bulk}} \left( \frac{2\pi k_B T}{k_{\text{harm}}} \right)^{3/2} e^{-[\Delta A_{\text{cavity}}^{0 \rightarrow 1} - \Delta A_{\text{bulk}}^{0 \rightarrow 1}]/k_B T}, \quad (14)$$

where the bulk density is  $\rho_{\text{bulk}} = N/V_{\text{bulk}}$ . A similar harmonic restraining potential was first introduced to serve as a reference thermodynamic state in a study of free energy of xenon in myoglobin (Hermans and Shankar, 1986).

The previous development can be generalized to derive similar expressions for  $R_n$ ,

$$R_n = \frac{1}{n} \rho_{\text{bulk}} \left( \frac{2\pi k_B T}{k_{\text{harm}}} \right)^{3/2} e^{-[\Delta A_{\text{cavity}}^{(n-1) \rightarrow n} - \Delta A_{\text{bulk}}^{0 \rightarrow 1}]/k_B T}, \quad (15)$$

where  $\Delta A_{\text{cavity}}^{(n-1) \rightarrow n}(r)$  corresponds to the free energy needed to insert one water molecule inside a cavity already containing  $(n-1)$  waters.

Once the quantities  $R_n$  have been calculated, the probability of occupancy is easily obtained from the normalization condition for  $P_n$  and the following relation:

$$\langle \delta_{n,n'} \rangle = \langle \delta_{0,n'} \rangle R_1 R_2 \cdots R_n, \quad (16)$$

giving

$$P_n = \frac{(R_1 R_2 \cdots R_n)}{1 + (R_1) + (R_1 R_2) + (R_1 R_2 R_3) + \cdots} \quad (17)$$

The probability that the cavity be unoccupied is

$$P_0 = \frac{1}{1 + (R_1) + (R_1 R_2) + (R_1 R_2 R_3) + \cdots} \quad (18)$$

All of the binding factors  $R_n$  and occupancy probabilities  $P_n$  are zero for  $n$  larger than  $N_{\text{max}}$ , the maximal number of water molecules that can be fitted into the cavity. An important special case occurs if the size of the cavity is such that it cannot be occupied by more than one water molecule. All of the factors  $R_2, \dots, R_n$  are then zero and the probability of finding one water inside the cavity is simply

$$P_1 = \frac{R_1}{1 + R_1}. \quad (19)$$

This equation can be compared with the familiar expression for first-order saturation for substrate binding:

$$P_1 = \frac{\rho_{\text{bulk}} K_1}{1 + \rho_{\text{bulk}} K_1}, \quad (20)$$

where  $\rho_{\text{bulk}}$  and  $K_1$  (by analogy with Eq. 14) play the role of the substrate concentration and binding constant, respectively.

Because they correspond to well-defined alchemical transformations between a first system with potential energy  $U_0 + u$  and a second system with potential energy  $U_1$ , the quantities  $\Delta A_{\text{cavity}}^{(n-1) \rightarrow n}$  can be calculated using the standard methodologies of free energy perturbation or thermodynamic integration (e.g., see Kollman, 1993, and references therein). Although the present formalism was developed in terms of a harmonic restraining potential, the analysis could easily be generalized to other kinds of potentials; e.g., Helms and Wade (1995) have recently used a flat-bottomed harmonic well to restrain the motion of a water molecule during a free energy perturbation. Alternatively, the restraining potential could also be applied to the center of mass of the inserted molecule. More importantly, although similar restraints have been used previously in free energy calculations (Hermans and Shankar, 1986; Chang and Hermans, submitted; Helms and Wade, 1995), the harmonic potential introduced here appears for the first time in rigorous mathematical expressions for the binding factors,  $R_n$ , and the probabilities of occupancy,  $P_n$ . Thus, the present theoretical formulation significantly clarifies the interpretation of free energy calculations for estimating the thermodynamic stability of water molecules in protein cavities.

Although the numerical value of  $\Delta A_{\text{cavity}}^{(n-1) \rightarrow n}$  depends on  $r^*$  and  $k_{\text{harm}}$ , the final result and the factor  $R_n$  are, in principle, independent of these quantities (see Eq. 13). For example, if the translational freedom of the water molecule confined in the harmonic well in the non-interacting system is smaller or larger than in the fully interacting cavity, the free energy  $\Delta A_{\text{cavity}}^{(n-1) \rightarrow n}$  will contain compensating contributions such that the final result for the factor  $R_n$  is unchanged. The restraining potential in the present formalism plays a role similar to the window potential in the umbrella sampling procedure of Patey and Valleau (1975); i.e., a biasing

potential is introduced to facilitate the computation and its influence is removed from the final result. However, independence from the harmonic potential and accuracy in the free energy analysis are conditional on accuracy in the evaluation of  $\Delta A_{\text{cavity}}^{(n-1) \rightarrow n}$ . An optimal choice of the parameters  $r^*$  and  $k_{\text{harm}}$  may be found by minimizing the contribution of the harmonic restraint to the free energy of binding. Taking the fully interacting system  $U_1$  as a reference, that is,

$$A(r^*, k_{\text{harm}}) = k_B T \ln \langle e^{u(r)/k_B T} \rangle_{(1)} + k_B T \ln \left[ \rho_{\text{bulk}} \left( \frac{2\pi k_B T}{k_{\text{harm}}} \right)^{3/2} \right], \quad (21)$$

the first term can be approximated to the lowest order in perturbation:

$$k_B T \ln \langle e^{u(r)/k_B T} \rangle_{(1)} \approx \langle u(r_1) \rangle_{(1)} \quad (22)$$

$$= \frac{1}{2} k_{\text{harm}} [\langle \delta r_1^2 \rangle_{(1)} + (\langle r_1 \rangle_{(1)} - r^*)^2],$$

where  $\langle \delta r_1^2 \rangle_{(1)}$  and  $\langle r_1 \rangle_{(1)}$  are, respectively, the mean square fluctuations and the average position of the oxygen of the (unrestrained) water molecule 1 in the system  $U_1$ . To find the optimal harmonic restraining potential, we seek to find the values of  $r^*$  and  $k_{\text{harm}}$ , which correspond to a minimum of  $A(r^*, k_{\text{harm}})$ , yielding

$$r^* = \langle r \rangle_{(1)} \quad (23)$$

and

$$k_{\text{harm}} = \frac{3k_B T}{\langle \delta r^2 \rangle_{(1)}}. \quad (24)$$

Thus, the optimal choice for the confining harmonic potential is that which best matches the average position and the mean square fluctuations of the unrestrained water molecule in the cavity during a dynamic simulation of the fully interacting system,  $U_1$ .

So far, the present methodology has been developed for a general case in which the waters filling the cavity can move freely and exchange their position during the particle insertion simulations. As waters embedded inside protein cavities are often loosely bound and can move over large volumes (as indicated in their large  $B$  factors), they are expected to influence each other's stability. Those effects are reflected in the formalism. As the  $n$ th water is being created (i.e.,  $\lambda$  is approximately zero), nothing prevents the already existing  $(n-1)$  waters to move into the empty space that the fully grown  $n$ th water would occupy. Such overlap is important to obtain the correct free energy estimate as expressed by Eq. 15. It is precisely as the  $n$ th water is influenced by the already existing  $(n-1)$  waters during the insertion that important free energy correlation effects are incorporated in the binding factors  $R_n$ . The expression derived for  $R_n$  requires that the configurational integral must be performed over all possible configurations during the free energy calculation  $\Delta A_{\text{cavity}}^{(n-1) \rightarrow n}$ . Thus, direct application of Eq. 15 is based on the assumption that the  $n$ th water molecule can exchange its position and mix with the  $(n-1)$  other molecules as it is being inserted in the cavity. This condition may not be respected in the case of a narrow channel, in which the water molecules have a single-file configuration and cannot pass one another. In such systems, the order of insertion will be maintained over all of the free energy calculations and the configurational integral yielding Eq. 15 will be incomplete. To determine the complete free energy of binding, it is therefore necessary to include a factor  $n!$  corresponding to the number of equivalent ways to fill the narrow channel. The origin of the  $n!$  in the case of a narrow channel can be explained by the following argument. By analogy with Eq. 12, the product  $R_1^{\text{cavity}} R_2^{\text{cavity}} \cdots R_n^{\text{cavity}}$  may be expressed as (the notation has been simplified slightly for the sake of clarity)

$$R_1^{\text{cavity}} R_2^{\text{cavity}} \cdots R_n^{\text{cavity}} \equiv R_{1-n}^{\text{cavity}} \quad (25)$$

$$= \frac{1}{n!} \int_{\text{cavity}} dx_1 dx_2 \cdots dx_n e^{-W(r_1, r_2, \dots, r_n)/k_B T},$$

where  $W(r_1, r_2, \dots, r_n)$  is the PMF corresponding to the configuration-dependent free energy required to insert  $n$  water molecules inside the cavity at the position  $(r_1, r_2, \dots, r_n)$ . The integration is totally unrestricted and the integrand runs over all possible values of  $r_1, r_2, \dots, r_n$ . Due to the indistinguishability of the water molecules, the PMF is invariant with respect to the exchange of water molecules; i.e.,  $W(r_1, r_2, \dots, r_n) = W(r_2, r_1, \dots, r_n)$  and so forth. Thus, the integration is taking place over many equivalent regions of configurational space. However, when the cavity is a long narrow channel, there can be large energy barriers (much larger than  $k_B T$ ) such that the water molecules cannot exchange their position during a simulation and are effectively confined along a one-dimensional axis. Assuming that the channel is oriented along the  $z$  axis, it is possible to arrange the four waters such that  $z_1 < z_2 < \dots < z_n$ , or any other order. Thus, the complete integral shown above can be expressed as

$$R_{1-n}^{\text{cavity}} = \frac{1}{n!} \int_{z_1 < z_2 < \dots < z_n} dr_1 dr_2 \dots dr_n e^{-W(r_1, r_2, \dots, r_n)/k_B T} + \dots$$

$$\frac{1}{n!} \int_{z_2 < z_1 < \dots < z_n} dr_1 dr_2 \dots dr_n e^{-W(r_1, r_2, \dots, r_n)/k_B T} + \dots$$
(26)

This is not as restricted as it may seem. The molecules are essentially ordered along the  $z$  axis because they do not exchange positions. However, this does not imply that they do not have motions and fluctuations in the  $x$  and  $y$  directions. There are  $n!$  equivalent integrals to account for all of the possible ways to introduce the  $n$  waters inside the channel, and the complete integral can be expressed as

$$R_{1-n}^{\text{cavity}} = \int_{z_1 < z_2 < \dots < z_n} dr_1 dr_2 dr_3 \dots dr_n e^{-W(r_1, r_2, \dots, r_n)/k_B T}$$
(27)

There is no such  $n!$  for the  $R^{\text{bulk}}$  factors as the waters in the bulk region can exchange their position freely and are totally uncorrelated (in the thermodynamic limit). In the case in which the water molecules are located along a narrow channel, it may be more effective to compute the free energy  $\Delta A_{\text{cavity}}^{0 \rightarrow n}$  directly for a given ordered configuration. Based on Eqs. 14, 15, and 16, the result of the free energy perturbation is then

$$R_{1-n}^{\text{cavity}} = (\rho_{\text{bulk}})^n \left( \frac{2\pi k_B T}{k_{\text{harm}}} \right)^{3n/2} e^{-[\Delta A_{\text{cavity}}^{0 \rightarrow n} - n\Delta A_{\text{bulk}}^{0 \rightarrow 1}]/k_B T},$$
(28)

where  $\Delta A_{\text{cavity}}^{0 \rightarrow n} = \Delta A_{\text{cavity}}^{0 \rightarrow 1} + \dots + \Delta A_{\text{cavity}}^{(n-1) \rightarrow n}$  is the free energy of insertion of  $n$  waters in an ordered configuration. For the sake of simplicity, it was assumed in deriving Eq. 28 that the optimal force constant  $k_{\text{harm}}$  of the confining harmonic potential is the same for the  $n$  ordered waters.

## Application to bacteriorhodopsin

All simulations on bR were performed using the CHARMM program (Brooks et al., 1983).

### Potential energy function and model system

**Potential energy function.** The form of the potential function used has been given elsewhere (Nina et al., 1995). It contains harmonic terms representing bond length and angle deformation and improper torsional displacements, a sinusoidal dihedral term, and pairwise-additive van der Waals and Coulombic electrostatic terms representing the interactions between non-bonded atoms. No explicit hydrogen-bonding terms are included; hydrogen bonds are modeled using electrostatic and van der Waals interactions. The PARAM22 potential function parameters were employed for the amino

acid residues (MacKerell et al., 1992). The TIP3P model was used to represent the water molecules (Jorgensen et al., 1983). Parameters for the protonated retinal have been derived using ab initio and semi-empirical quantum chemistry calculations on water-Schiff base hydrogen-bonded complexes (Nina et al., 1993, 1995). Nonbonded interactions were brought to zero using a group-based switching function between 10 and 12 Å. All covalent bonds involving hydrogen atoms were kept fixed with the SHAKE algorithm (Ryckaert et al., 1977). The adopted basis Newton-Raphson algorithm was used for all energy minimizations (Brooks et al., 1983). Molecular dynamics calculations were performed with a timestep of 2 fs.

**Model system.** The system modeled is light-adapted bR<sub>568</sub>. In this species, the retinal is all-*trans* and protonated (Harbison et al., 1984a,b; Smith et al., 1989). The model was derived from the structure of bR determined experimentally using electron microscopy. The resolution is approximately 3 Å in the direction parallel to the membrane plane and almost 7 Å in the direction perpendicular to the membrane plane (Henderson et al., 1990). The experimental coordinates were modified in the following ways (Zhou et al., 1993; Humphrey et al., 1994; Nina et al., 1995). First, the position of helix D (residue 106–127) was translated by 4 Å in the + $Z$  direction, i.e., toward the cytoplasmic side of the membrane (Henderson, personal communication). Second, the inter-helical loops were modeled and added to the seven transmembrane helices so as to approximately incorporate their influence on the global structure and dynamics (Ferrand et al., 1993). Residues 1–7 were not included. The details of the conformation of the loops are not expected to significantly influence the present results as they are located far away from the Schiff base. Third, the hydrogens were added using the HBUILD command of CHARMM (Brunger and Karplus, 1988).

The protonation state of the ionizable groups was assigned on the basis of experimental measurements and theoretical  $pK_a$  calculations (Lewis et al., 1978; Doukas et al., 1981; Druckmann et al., 1982; Engelhard et al., 1985; Gerwert et al., 1987; Subramaniam et al., 1990; Herzfeld et al., 1990; Bashford and Gerwert, 1992). The residues Asp 85 and Asp 212 were unprotonated whereas Asp 96 and Asp 115 were protonated (Braiman et al., 1988; Gerwert et al., 1989, 1990). By default, the internal residues Glu 9 and Glu 204 were unprotonated and Arg 82 was protonated as no experimental data are available for these residues. The Tyr residues 57, 79, 83, and 185 were protonated.

### Positioning of the water molecules

Previous quantum chemical results indicate that water molecules can form strong hydrogen bonds with the retinal Schiff base at two positions, as illustrated in Fig. 1 (Nina et al., 1995). In one position, a water molecule, which we label molecule A, hydrogen bonds with the N16-H16 group of the retinal on the extracellular side of the Schiff base, in a polar hydrophilic cavity. In the other position, a water molecule (molecule B) hydrogen bonds to the retinal C15-H15 group in a relatively hydrophobic region on

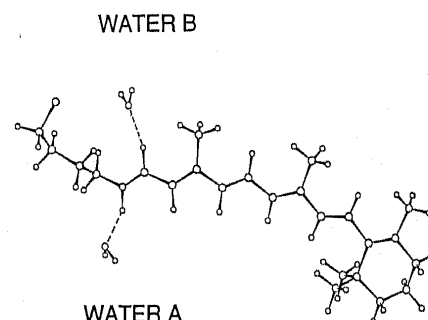


FIGURE 1 Arrangement of water molecules hydrogen bonded to a protonated Schiff base obtained by ab initio quantum chemical calculations after insertion into the bR structure and energy minimization (Nina et al., 1995).

the cytoplasmic side of the Schiff base (Nina et al., 1995). Energy minimization calculations suggested that two water molecules can be incorporated in bR in sites A and B without significantly perturbing the protein structure. In the present work, water molecules A and B were incorporated in their respective sites following the minimization protocol described in Nina et al., 1995.

The simulations indicated that four water molecules, with interoxygenn distances of  $\sim 2.8$  Å, can form a continuous hydrogen-bonded chain between the Asp 96 side-chain and the Schiff base in the nonpolar channel. One of these molecules, which hydrogen bonded to the CH group of the Schiff base, is molecule B. If there are less than four molecules in the nonpolar channel they cannot form a continuous chain because the distance between Asp 96 and the Schiff base is 10–12 Å. Molecular dynamics calculations using five or more water molecules in the channel led to severe disruption of the protein. Therefore, in addition to waters A and B, three more water molecules were inserted into the nonpolar channel (water molecules C, D, and E). Waters B, C, D, and E form the continuous hydrogen-bonded chain from Asp 96 to the Schiff base. Water molecules A–E are the subjects of the thermodynamic calculations in this paper. An additional 23 water molecules were added to the polar channel on the extracellular side of the Schiff base; 5 of these are disposed in single file approximately along the axis defined by water molecule A and the Glu 204 side-chain, and 17 water molecules lie on the extracellular side of Glu 204. Hereafter, the resulting model is referred to as system I.

The positions of the water molecules in system I were refined using a series of energy minimizations and molecular dynamics calculations. During the initial calculations, water molecules A and B and all the protein atoms were fixed and harmonic distance restraints were applied between the oxygens of successive water molecules to maintain the configuration of the hydrogen-bonded single-file chain in the hydrophobic and hydrophilic channels. After a few refinement cycles with the protein and waters A and B fixed, all atoms closer than 16 Å from the N16 of the Schiff base were restrained using a harmonic potential while all of the remaining atoms were kept fixed. Several more cycles of energy minimization and molecular dynamics were then used to relax the structure, during which the force constants of the harmonic restraints were progressively reduced until all of the atoms within 16 Å were free to move. The hydrated protein model resulting from the refinement protocol was then equilibrated for 40 ps using molecular dynamics with velocity rescaling.

To investigate the thermodynamic stability of the water hydrogen bonding to the retinal C15-H15 group (water B), a second model (system II) was generated in which the three water molecules (C, D, and E) located in the nonpolar channel were removed, leaving water molecule B hydrogen bonded to the retinal CH group. After a short initial energy minimization, system II was equilibrated for 40 ps.

The present simulations were performed in the absence of explicit lipid, bulk water, or neighboring protein molecules. It has been observed that bR has a tendency to take a globular shape under these conditions (Nonella et al., 1991; Ferrand et al., 1993). Therefore, all backbone atoms of residues farther than 18 Å from the NH of the Schiff base were restrained using a harmonic potential with a force constant of 2 kcal/mol/Å<sup>2</sup>. Although distortions were reduced in simulations of the full bR trimer in an explicit solvent and lipid membrane environment (Edholm et al., 1995), the present free energy simulations would not be computationally tractable using such a large simulation system (>18,000 atoms). In addition, the entire solvent-membrane system is not necessary for the present calculations. This is because the dominant contribution to Eq. 13 arises from local water-protein interactions in the proton channel near the Schiff base. The contributions from the long-range interactions with the surrounding solvent and lipid are expected to be negligible; e.g., the free energy arising from the interaction of a water dipole in a cavity of 15 Å radius embedded in a continuum dielectric, calculated using the Onsager equation (Onsager, 1936) is only  $\sim 0.01$  kcal/mol. Thus, the neglect of the membrane environment and the application of protein harmonic restraints are not expected to influence significantly the thermodynamic results of the present study.

## Free energy simulations

In Eq. 13,  $\Delta A_{\text{cavity}}^{0 \rightarrow 1}$  is the free energy difference between a system with potential energy  $U_1$ , in which a fully interacting water molecule is free to move inside the cavity and a system with potential energy  $U_0 + u$ , in which the water molecule is non-interacting and harmonically restrained by the potential  $u(r)$ . Although the calculation of  $\Delta A_{\text{cavity}}^{0 \rightarrow 1}$  could in principle be performed in a single step, it is advantageous to calculate the contributions from the long-range electrostatic and short-range van der Waals interactions separately. One reason for this is that these terms have different convergence characteristics; for example, the harsh van der Waals repulsion must be treated with care (Zacharias et al., 1994, and references therein). Another reason for adopting a two-step procedure is that physical insight can be gained into the van der Waals and electrostatic contributions to the free energy differences. Decomposition of the free energy is path dependent (Shi et al., 1993). However, when used with care and with an appropriate choice of path, a decomposition can give useful information on the role of individual terms in the energy function (Borech et al., 1994).

To treat the electrostatic and Lennard-Jones contributions separately, the free energy differences were calculated in two steps. A path was chosen involving an intermediate system in which a water molecule with neutral atoms is restrained by the potential  $u(r)$ . In the intermediate state, the partial charges of the TIP3P model were set to zero whereas the Lennard-Jones parameters were conserved. In the first step, the free energy,  $\Delta A^{\text{vdw}}$ , corresponding to turning on the Lennard-Jones interactions of a neutral water restrained by the potential  $u(r)$  was calculated. This is the contribution due to van der Waals interactions,  $\Delta A^{\text{vdw}}$ , to the free energy  $\Delta A_{\text{cavity}}^{0 \rightarrow 1}$ . It was calculated using the slow growth method (Singh et al., 1987) in which the thermodynamic integration is performed as a function of time along a trajectory of 50 ps. The free energy was estimated from forward and backward perturbations. The initial state was defined for the system in which the van der Waals radii and the atomic partial charges of water were set to zero. The restraint  $u(r)$  was applied to the oxygen atom of the water molecule(s) concerned with a force constant of 20 kcal/mol/Å<sup>2</sup>. The reference positions of the harmonic potentials used in the free energy calculations are given in Table 1. The force constant and the origin of the potential were obtained by applying Eqs. 23 and 24 to the positions and fluctuations obtained from the equilibration molecular dynamics run (the rms fluctuations of all of the waters was on the order of 0.3 Å).

The second step corresponds to the contribution due to electrostatic interactions and the harmonic restraint  $\Delta A^{\text{elec} + \text{harm}}$  to the free energy  $\Delta A_{\text{cavity}}^{0 \rightarrow 1}$ . In practice, the computation of the  $\Delta A^{\text{elec} + \text{harm}}$  terms involves gradually turning on the charges of a water molecule while turning off the harmonic confining potential,  $u(r)$ .  $\Delta A^{\text{elec} + \text{harm}}$  was calculated using the perturbation windowing thermodynamic integration method (Kirkwood, 1935; Kollman, 1993) with 10 intermediate trajectories generated at values of the coupling parameter  $\lambda = 0.05, 0.15, \dots, 0.95$  that were perturbed by  $\pm 0.05$  to obtain the free energy increments  $\Delta A^{\text{elec} + \text{harm}}(\lambda, \lambda + \delta\lambda)$ . The simulation for each window was equilibrated for 0.5 ps, starting from the last configuration of the previous window. The sampling was performed for 2 ps for each  $\lambda$ . The free energy was estimated from forward and backward simulations.

All of the free energy simulation trajectories were generated with Langevin dynamics at a temperature of 300K. The nonhydrogen atoms

TABLE 1 Reference for the harmonic potentials

Water	Reference positions (Å)		
	$x_0$	$y_0$	$z_0$
A	15.7	−9.9	3.9
B	15.4	−7.4	10.0
C	15.8	−9.4	11.9
D	15.8	−11.3	13.8
E	16.1	−10.5	16.4

The Schiff base N<sub>ε</sub> of Lys 216 is located at (16.6, −9.0, 6.6) and the protonated O<sub>δ2</sub> of Asp 96 is located at (13.5, −9.4, 18.2).



were submitted to weak dissipative and stochastic Langevin forces corresponding to a velocity relaxation rate of  $5 \text{ ps}^{-1}$ . The stochastic dynamics was used to ensure that the statistical configurational sampling corresponded to that of a Boltzmann distribution characteristic of a canonical ensemble at 300 K. All of the free energy calculations were done using the PERT facility of CHARMM.

The thermodynamics of three hydration states of the proton channel near the Schiff base were investigated. The polar channel (NH side, below the Schiff base) and the nonpolar channel (CH side, above the Schiff base) are treated as two separate, noncommunicating cavities. Molecular dynamics calculations starting from the equilibrated system I were used to evaluate the free energy for inserting water molecule A and the free energy for simultaneously inserting water molecules B, C, D, and E together. Molecules B–E were inserted together because it was found in the simulations that they do not pass one another and exchange their positions in the narrow hydrophobic channel. Molecular dynamics calculations starting from the equilibrated system II were performed to calculate the free energy of inserting water molecule B in the absence of the water molecules C, D, and E in the nonpolar channel.

The free energy calculations for the three hydration states required a total simulation time of 300 ps, i.e., 50 ps for each of the two steps for each forward and backward transformation. This took approximately 1 month on a single CPU of a Silicon Graphics SGI/480 Power Series computer. Although additional and longer simulations could be generated to improve the statistical convergence and accuracy of the present free energy calculations, the latter is only one part of the uncertainty due to the low resolution of the electron microscopy structure.

## RESULTS

The results of the thermodynamic calculations on bR are given in Table 2. First, we consider the polar cavity on the extracellular side of the Schiff base, occupied by water molecule A in the simulation. As the polar cavity can at most contain one water molecule, only the binding factor  $R_1$  is required for a discussion of the occupancy probabilities. The calculated free energy  $\Delta A_{\text{cavity}}^{0 \rightarrow 1}$  for insertion of water A is  $-13.8 \text{ kcal/mol}$ . In comparison, the free energy difference  $\Delta A_{\text{bulk}}^{0 \rightarrow 1}$  obtained for inserting a TIP3P water molecule in pure water is  $-6.4 \text{ kcal/mol}$  (Beglov and Roux, 1994). The above values yield a binding factor  $R_1$  of 667. Based on Eq. 19, the calculated probability of occupancy is  $667/(667 + 1) = 0.998$ . This indicates that there is effectively full occupancy of the water molecule in the polar cavity. The calculated free energy for water A results from a large electrostatic contribution ( $-19.3 \text{ kcal/mol}$ ), which is partly canceled by a significant van der Waals contribution ( $+5.4 \text{ kcal/mol}$ ). The size of the electrostatic contribution can be easily understood as water A simultaneously forms hydrogen bonds to the Schiff base NH and to the  $\text{O}_\delta$  atoms of both Asp 85 and Asp 212. A snapshot of the hydrogen bond network in the cytoplasmic side of the channel, taken after 40 ps of equilibration, is shown in Fig. 2. During the equilibration, the average  $\text{H}_2\text{O} \cdots \text{HN}$  distance for the hydrogen bond was  $2.03 \text{ \AA}$  and the associated RMS fluctuation  $0.30 \text{ \AA}$ . Thus, water A is well localized in the simulation due to its strong hydrogen bonds. Other hydrogen bonds in the polar region near the Schiff base are observed, in particular  $\text{H}_\eta$  of Tyr 57 and  $\text{H}_\epsilon$  of Trp 86 with  $\text{O}_\delta$  of Asp 212 and  $\text{H}_\gamma$  of Thr 89 with  $\text{O}_\delta$  of Asp 85. Arg 82 is farther from water A and hydrogen bonds to other water molecules in the hydrophilic channel.

Interestingly, the strong polar interactions present in the environment of the Schiff base are probably at the origin of the large van der Waals free energy contribution. The van der Waals contribution corresponds to free energy changes on insertion into site A of a Lennard-Jones sphere representing a water molecule with no charges. Changes in the geometry of the environment during the insertion of the sphere lead to contributions to the free energy. In the present case, favorable interactions involving the Schiff base, Asp 212, Asp 85, and Trp 86 are lost when water A is inserted. In particular, a hydrogen bond is observed between the  $\text{O}_\delta$  of Asp 212 and the Schiff base NH group at  $\lambda = 0.05$  and at  $\lambda = 0.00$ , i.e., near and at the end-point simulation in which the uncharged water molecule is not coupled with its surroundings. The loss of this hydrogen bond during the insertion of the sphere will contribute a significantly unfavorable free energy. The contribution to the free energy

of the Schiff base are probably at the origin of the large van der Waals free energy contribution. The van der Waals contribution corresponds to free energy changes on insertion into site A of a Lennard-Jones sphere representing a water molecule with no charges. Changes in the geometry of the environment during the insertion of the sphere lead to contributions to the free energy. In the present case, favorable interactions involving the Schiff base, Asp 212, Asp 85, and Trp 86 are lost when water A is inserted. In particular, a hydrogen bond is observed between the  $\text{O}_\delta$  of Asp 212 and the Schiff base NH group at  $\lambda = 0.05$  and at  $\lambda = 0.00$ , i.e., near and at the end-point simulation in which the uncharged water molecule is not coupled with its surroundings. The loss of this hydrogen bond during the insertion of the sphere will contribute a significantly unfavorable free energy. The contribution to the free energy

TABLE 2 Results of the free energy simulations

Simulations		Free energies (kcal/mol)				Total
		vdW	Elec + Harm	Elec	Harm	
Water A in system I	F		-18.9	-17.6	-1.3	-13.8
	B		19.6	17.9	1.7	
	F	5.9				
	B	-4.9				
Water BCDE in system I	F		-39.1	-33.2	-5.9	-37.6
	B		38.0	32.2	5.8	
	F	0.8				
	B	-1.1				
Water B in system II	F		-13.2	-12.1	-1.2	-13.8
	B		12.6	11.0	1.5	
	F	-1.0				
	B	0.7				

F, forward trajectory; B, backward trajectory; vdW, van der Waals.

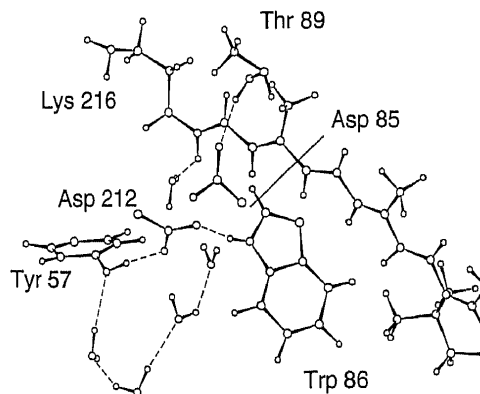


FIGURE 2 Configuration resulting from the construction of water molecules in the hydrophilic proton channel after equilibration from molecular dynamics. A water molecule (water A) directly hydrogen bonded to the NH of the Schiff base and a few of the water molecules located in the hydrophilic channel belonging to the extracellular bulk region are shown (most of the 23 water molecules located in the hydrophilic channel between the Schiff base and Glu 204 are not shown).

change from the harmonic restraining potential is approximately +1.5 kcal/mol, which is close to the optimal value of  $\frac{1}{2}k_B T$  according to Eqs. 22, 23, and 24.

Second, the nonpolar cavity is considered. Based on its size, the nonpolar cavity can in principle contain from zero to four water molecules. The free energy of insertion of a first water on the cytoplasmic side of the Schiff base was calculated by performing a thermodynamic calculation for the insertion of water molecule B in system II. This yields an estimate of the first binding factor  $R_1$  for this cavity. Although a complete sampling over the whole nonpolar cavity is formally required to calculate the binding factor  $R_1$ , the insertion of a first water forming a hydrogen bond to the CH of the Schiff base picks up the dominant contribution arising from the most stable position for a first water in the nonpolar channel. The calculated binding free energy for water B is -13.8 kcal/mol, the same value as for water A. Consequently, the calculated probability of occupancy is again 0.998. However, the contributions to the free energy of insertion of waters A and B are significantly different. The electrostatic contribution is less favorable for insertion of water B whereas the van der Waals contribution is more favorable. This is primarily due to the fact that the cavity containing water B is already preformed in the absence of the water molecule and no significant free energy is required for inserting a particle (neutral water B) at this position. Water B is located in a narrow region of the channel, far from the cytoplasmic protein surface. It forms hydrogen bonds with both the retinal CH group and the backbone carbonyl oxygen of Thr 89 that persist in the simulations. The average distance between the oxygen atom of water B and the hydrogen of the retinal CH group was 2.15 Å and the associated RMS fluctuation 0.18 Å during the equilibration dynamics. This is consistent with previous calculations indicating that this  $\text{CH} \cdots \text{O}$  has a strong interaction energy (Nina et al., 1995). As in the case of water A, the contribution from the harmonic restraining potential is near the optimal limit of  $\frac{1}{2}k_B T$ .

The thermodynamic stability of the column of four water molecules BCDE in the nonpolar channel was also examined. The binding free energy  $\Delta A_{\text{cavity}}^{0 \rightarrow 4}$ , corresponding to the reversible thermodynamic work needed to simultaneously insert a single file of four waters into the channel, calculated using system I, is -37.6 kcal/mol. This free energy is significantly more negative than the free energy for insertion of four waters in bulk water ( $-6.4 \times 4 = -25.6$  kcal/mol). The channel on the cytoplasmic side is mostly lined by nonpolar residues from helices B (residue 38–62), C (residues 74–100), and G (residues 202–225). In particular, helix C has a long stretch of nonpolar residues leading from the cytoplasmic side to the retinal: Thr 89, Thr 90, Pro 90, Leu 92–95, Asp 96, Leu 97, Ala 98, Leu 99–100, and Val 101. The residues Phe 219, Ile 220, Leu 221, Ile 222, and Leu 223 of helix G line the entrance of the channel. Water molecules BCDE are in contact with the side chains of Thr 46, Val 49, Pro 50, Thr 89, Leu 93, Phe 219, Ile 220, and Leu 223. Thus, the four waters in the channel are not in contact with polar side-chains. The question arises, therefore, as to the origin of the stabilization free energy in the channel. Table 2 indicates that the free energy of insertion of the column is dominated by the electrostatic contribution. Indeed, as well as the above-mentioned factors stabilizing water molecule B, the four water molecules form hydrogen bonds between themselves and with neighboring backbone groups. The hydrogen bonds present in the BCDE system are depicted in Fig. 3. The four water molecules form a continuously hydrogen-bonded single file with water B and E hydrogen bonding to the retinal CH group and to the  $\text{O}_{\gamma 2}$  of Asp 96, respectively. In addition, waters B, C, and D are hydrogen bonded to the backbone carbonyl oxygens of Thr 89, Lys 216, and Ala 215, respectively. The hydrogen-bonding network and the single file of waters was intact during both the equilibration period and the free energy calculations.

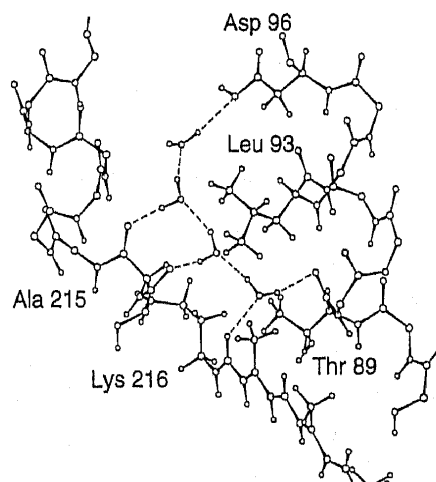


FIGURE 3 Configuration resulting from the construction of water molecules in the hydrophobic proton channel after equilibration from molecular dynamics. Water B (bottom), C, D, and E (top) are shown. Water B is hydrogen bonded to the retinal CH group. The cavity concerns mostly residues from helix C (74–100), e.g., Thr 89, Leu 93, and Asp 96, and helix G (202–225), e.g., Ala 215 and Lys 216.



The presence of water in the channel does not significantly perturb the geometry of the protein. All of the backbone  $(i)\text{-C=O}\cdots\text{H-N}(i+4)$   $\alpha$ -helical hydrogen bonds remain intact except for that between Ala 215 and Phe 219, which is broken due to the interaction of Ala 215 with water D. The side chain of Leu 93 is the cause of a significant steric hindrance on the proton transfer pathway. As a result, as can be seen from Fig. 3, waters C, D, and E deviate from a linear configuration. This suggests that substitution of Leu 93 by a residue with a smaller side-chain would significantly affect the arrangement of water molecules connecting Asp 96 to the Schiff base.

The calculated binding free energy for the four molecules yields a binding factor,  $R_{1-4}$ , of 0.03. This is much smaller than the binding factor obtained for water molecule A or water molecule B. This indicates that these water molecules are likely to have a marginal stability in the nonpolar channel. Therefore, the four-molecule, hydrogen-bonded chain might be expected to yield a partial occupancy. Although the binding factors  $R_2$  and  $R_3$  are needed for a complete discussion of the thermodynamic stability of the water occupancy, those were not calculated due to the computational limitations. Thus, the probability of occupancy,  $P_n$ , cannot be evaluated for  $n = 1, 4$ . However, the fact that the free energy of transfer of the column of water from the bulk to the channel is significantly negative indicates that the transfer of a column of water molecules from bulk water to the cytoplasmic channel of bR is thermodynamically permitted. Experimentally, it has been observed that the reaction involving the transfer of a proton from Asp 96 to the Schiff base is affected by the presence of osmotically active solutes and perturbants and can be specifically inhibited by withdrawing water molecules from the inside of the protein (Cao et al., 1991). The experimentally observed sensitivity to the osmolarity of the bulk solution suggests, in qualitative agreement with the present calculations, that the stability of those internal water molecules that participate in the proton transfer reaction might be marginal.

## CONCLUDING DISCUSSION

The thermodynamic stability of water molecules in the bR proton channel was investigated using molecular dynamics simulations and free energy calculations. Following the approach of Wade et al. (1990, 1991), a theoretical framework for estimating the thermodynamic stability of water molecules inside an isolated cavity buried in the interior of a protein was formulated and rigorous mathematical expressions that can be evaluated from computer simulations were derived for calculating the binding constant and the probability of water occupancy in specific sites. This novel theoretical development and the present free energy simulations allow a quantitative discussion of the hydration of buried water sites in bR.

The application of the theory to the thermodynamic stability of water molecules in the proton transfer channel of

bR provides an example of the use of the method to answer specific fundamental questions arising from experimental work. The presence of one or more water molecules in the vicinity of the Schiff base has been suggested from several experiments. A resonance Raman study indicates that a negatively charged complex counterion, formed by the proton acceptor Asp 85, Asp 212, and probably Arg 82, is stabilized by water molecules near the Schiff base group (Hildebrandt and Stockburger, 1984). Solid state  $^{13}\text{C}$  and  $^{15}\text{N}$  nuclear magnetic resonance (NMR) experiments led to a model being proposed in which a water molecule is directly hydrogen-bonded to the Schiff base NH group (De Groot et al., 1990). Additional solid state  $^1\text{H}$  and  $^{15}\text{N}$  NMR experiments suggest that there is a direct exchange of the Schiff base NH hydrogen with bulk water (Harbison et al., 1988). More recently, a resonance Raman study of the Schiff base hydrogen/deuterium exchange also led to the conclusion that a water molecule is directly hydrogen-bonded to the Schiff base NH group (Deng et al., 1994) and a Fourier transform infrared difference spectroscopy study concluded that two water molecules are trapped near the bR active site (Fischer et al., 1994).

The present free energy results indicate that water molecules A and B, which hydrogen bond directly to the retinal Schiff base, are thermodynamically stable. During the simulations, these water molecules stay hydrogen-bonded in their respective NH and CH sites. Consequently, hydrolysis of the Schiff base into the tertiary amine and the retinal aldehyde via attack of the  $\pi$ -electrons at the  $\text{N}=\text{C}$  by a water molecule, which occurs rapidly in bulk solution, is prevented in bR because the hydrogen-bonded water molecules cannot move into a position perpendicular to the retinal plane. Water molecule A simultaneously forms hydrogen bonds to the Schiff base NH and the  $\text{O}_\delta$  of Asp 85 and Asp 212 in the simulation. Mutational analyses confirm the strong catalytic function of Asp 85 and Asp 212 in the retinal photoisomerization process in bR (Song et al., 1993). Fourier transform infrared spectroscopy has indicated the presence of a water-Asp 85 interaction (Maeda et al., 1994).

The present calculations suggest that the thermodynamic stability of water molecule B is approximately the same as that of water molecule A. Water molecule B forms a relatively unusual  $\text{CH}\cdots\text{O}$  hydrogen bond that is stabilized by delocalization of the positive charge of the protonated Schiff base (Nina et al., 1995). It has been suggested that one reason why the primary isomerization does not occur around the N-C15 bond during the retinal photocycle might be that the configuration of the water molecules around the Schiff base shields the positive charge on C15 in the photoexcited state (Song et al., 1995). Appropriate isotope-labeling spectroscopic experiments aimed at detecting a water molecule hydrogen-bonded to the retinal CH group would seem to be worth undertaking. Based on the present model, the carbon-water distance between the retinal carbon C20 (methyl group) and water molecule B is on the order of 3.2 Å. This suggests that a possible experiment would be to use solid-state NMR to detect magnetization transfer be-

tween  $^{13}\text{C}$ -labeled retinal at the C20 carbon position and  $^{17}\text{O}$ -labeled water.

Water molecules such as A and B, directly associated with the Schiff base, may significantly perturb the electronic structure of retinal (Hildebrandt and Stockburger, 1984; Beppu et al., 1994) and could play other important roles in the bR photocycle. Experiments using synthetic retinal protonated Schiff bases lend support to the idea that water molecules hydrogen-bonded to the Schiff base can modulate the  $\text{pK}_a$  of the NH group (Gat and Sheves, 1993). Quantum chemical calculations on Schiff base/water/counterion complexes suggest that the presence of water is indispensable for the existence of the Schiff base in the protonated form, i.e., the direct Schiff base/carboxylate ion pair is energetically unstable compared with the neutral complex (Beppu et al., 1992). Continuum electrostatic calculations suggest that a water molecule hydrogen-bonded directly to the Schiff base NH may determine the  $\text{pK}_a$  of adjacent residues (Sampogna and Honig, 1994). Molecular dynamics calculations suggest that the presence of water molecules near the Schiff base can influence the dynamics of the isomerization of the retinal in the early stages of the photocycle (Zhou et al., 1993). The above considerations indicate that it has become clear that a detailed understanding of water-Schiff base hydrogen bonding will be required for a complete description of bR function.

The present results also indicate that the presence of a column of four water molecules in the nonpolar region of the channel between Asp 96 and the Schiff base is thermodynamically allowed. Water B is quite stable whereas the three other water molecules CDE in the hydrophobic channel have a marginal stability. The lack of resolution of the electron microscopy structure, in particular the uncertainty of the side-chain conformations, makes it difficult to address this question further by performing more accurate calculations and may have contributed to the marginal stability of the waters CDE in the hydrophobic channel. The free energy of insertion of the column of water molecules in the bR channel is significantly lower than that for their insertion in bulk water. The probability of occupancy is significantly less than one and might be sensitive to the presence of osmotically active solutes in the bulk solution (such as high salt concentration). The stabilization free energy is essentially electrostatic in origin and arises in part from the ability of the water molecules to make hydrogen bonds with themselves and the protein backbone carbonyl groups. The presence of water molecules in the cytoplasmic channel is consistent with results from low-resolution neutron scattering experiments (Zaccai, 1987; Papadopoulos et al., 1990). The present simulations are also in general accord with the results of molecular dynamics calculations using a slightly different potential function (Humphrey et al., 1994).

During the last steps of the photocycle, a proton is transferred from the side chain of Asp 96 to reprotonate the Schiff base (Gerwert et al., 1989). The present results lend support to the idea that water molecules play a direct role in

this process (Cao et al., 1991). Indeed, a water proton transfer chain may function even if it is incomplete for a significant fraction of the time, as suggested here. However, the present calculations were made on the light-adapted bR<sub>568</sub>. The proton transfer itself takes place in a different species in the photocycle (the M  $\rightarrow$  N step), in which the Schiff base is unprotonated and 13-*cis*. This may significantly affect the hydrogen-bonding pattern in the vicinity of the Schiff base. Indeed, evidence exists for changes in water-Schiff base hydrogen bonding during the photocycle (Fischer et al., 1994). Moreover, there is also evidence for structural changes in the protein in the M state (Subramaniam et al., 1993). More detailed experimental information on these aspects would aid in the setting up of reliable thermodynamic calculations on the bR photocycle intermediates.

The present theoretical development allows a quantitative discussion of the hydration of buried water sites in light-adapted bR. The finding that the presence of water molecules in an apparently hydrophobic region of a protein is thermodynamically permissible suggests that calculations such as those presented here may find widespread use. Moreover, the rigorous methodology presented here is generally applicable to the problem of estimating the thermodynamic stability of any small molecule in a specific site inside a macromolecule.

We are grateful to one reviewer who made many insightful comments. B. Roux is supported by grants from the Medical Research Council of Canada and from the Fonds pour la Recherche en Santé du Québec. We acknowledge support from NATO grant 920093. J. C. Smith acknowledges the Commissariat à l'Énergie Atomique for financial support.

## REFERENCES

- Bashford, D., and K. Gerwert. 1992. Electrostatic calculations of the  $\text{pK}_a$  values of ionizable groups in bacteriorhodopsin. *J. Mol. Biol.* 224: 473–486.
- Beglov, D., and B. Roux. 1994. Finite representation of an infinite bulk system: solvent boundary potential for computer simulations. *J. Chem. Phys.* 100:9050–9063.
- Beppu, Y., and T. Kakitani. 1994. Theoretical study of color control mechanism in retinal proteins. I. Role of the tryptophan residue, tyrosine residue, and water molecule. *Photochem. Photobiol.* 59(6):660–669.
- Beppu, Y., T. Katakini, and F. Tokunaga. 1992. Energetics of protonation-deprotonation of the chromophore in retinal proteins. *Photochem. Photobiol.* 56:1113–1117.
- Boresch, S., G. Archontis, and M. Karplus. 1994. Free energy simulations: the meaning of the individual contributions from a component analysis. *Proteins*. 20:25–33.
- Braiman, M. S., T. Mogi, T. Marti, L. J. Stern, H. G. Khorana, and K. J. Rothschild. 1988. Vibrational spectroscopy of bacteriorhodopsin mutants: light-driven proton transport involves protonation changes of aspartic acid residues 85, 96, and 212. *Biochemistry*. 27:8516–8520.
- Brooks, B. R., R. E. Bruccoleri, B. D. Olafson, D. J. States, S. Swaminathan, and M. Karplus. 1983. CHARMM: a program for macromolecular energy minimization and dynamics calculations. *J. Comp. Chem.* 4:187–217.
- Brooks, C. L. III, M. Karplus, and B. M. Pettitt. 1988. Proteins: a Theoretical perspective of dynamics structure and thermodynamics. In *Advances in Chemical Physics*, Vol. LXXI. I. Prigogine and S. A. Rice, editors. John Wiley & Sons, New York.

- Brunner, A. T., and M. Karplus. 1988. Polar hydrogen positions in proteins: empirical energy placement and neutron diffraction comparison. *Proteins*. 4:148-156.
- Butt, H. J., K. Fendler, E. Bamberg, J. Tittor, and D. Oesterhelt. 1989. Aspartic acids 96 and 85 play a central role in the function of bacteriorhodopsin as a proton pump. *EMBO J.* 8:1657-1663.
- Cao, Y., G. Váró, M. Chang, B. Ni, R. Needleman, and J. K. Lanyi. 1991. Water is required for proton transfer from Asp 96 to the bacteriorhodopsin Schiff base. *Biochemistry*. 30:10972-10979.
- De Groot, H. J. M., S. O. Smith, J. Courtin, E. van der Berg, C. Winkel, J. Lugtenburg, R. G. Griffin, and J. Herzfeld. 1990. Solid-state  $^{13}\text{C}$  and  $^{15}\text{N}$  NMR study of the low pH forms of bacteriorhodopsin. *Biochemistry*. 29:6873-6882.
- Deng, H., L. Huang, R. Callender, and T. Ebrey. 1994. Evidence for a bound water molecule next to the retinal Schiff base in bacteriorhodopsin and rhodopsin: a resonance Raman study of the Schiff base hydrogen/deuterium exchange. *Biophys. J.* 66:1129-1136.
- Desinov, V. P., B. Halle, J. Peters, and H. D. Horlein. 1995. Residence times of the buried water molecules in bovine pancreatic trypsin inhibitor and its G36S mutant. *Biochemistry*. 34:9046-9051.
- Doukas, A. G., A. Pande, T. Suzuki, R. H. Callender, B. Honig, and M. Ottolenghi. 1981. On the mechanism of hydrogen-deuterium exchange in bacteriorhodopsin. *Biophys. J.* 33:275-280.
- Druckmann, S., M. Ottolenghi, A. Pande, J. Pande, and R. H. Callender. 1982. Acid-base equilibrium of the Schiff base in bacteriorhodopsin. *Biochemistry*. 21:4953-4959.
- Edholm, O., O. Berger, and F. Jähnig. 1995. Structure and fluctuations of bacteriorhodopsin in the purple membrane: a molecular dynamics study. *J. Mol. Biol.* 250:94-111.
- Edsall, J. T., and H. A. McKenzie. 1983. Water and proteins. II. The location and dynamics of water in protein systems and its relation to their stability and properties. *Adv. Biophys.* 16:53-183.
- Engelhard, M., K. Gerwert, B. Hess, W. Kreutz, and F. Siebert. 1985. Light-driven protonation changes of internal aspartic acids of bacteriorhodopsin: an investigation by static and time-resolved infrared difference spectroscopy using  $[4-^{13}\text{C}]$  aspartic acid labeled purple membrane. *Biochemistry*. 24:400-407.
- Ferrand, M., G. Zaccari, M. Nina, J. C. Smith, C. Etchebest, and B. Roux. 1993. Structure and dynamics of bacteriorhodopsin: comparison of experiment and simulation. *FEBS Lett.* 327:256-260.
- Fischer, W. B., S. Sonar, T. Marti, H. G. Khorana, and K. J. Rothschild. 1994. Detection of a water molecule in the active site of bacteriorhodopsin: hydrogen bonding changes during the primary photoreaction. *Biochemistry*. 33:12757-12762.
- Gat, Y., and M. Sheves. 1993. A mechanism for controlling the  $\text{pK}_a$  of the retinal protonated Schiff base in retinal proteins: a study with model compounds. *J. Am. Chem. Soc.* 115:3772-3773.
- Gerwert, K., U. M. Ganter, F. Siebert, and B. Hess. 1987. Only water-exposed carboxyl groups are protonated during the transition to the cation-free bacteriorhodopsin. *FEBS Lett.* 213:39-44.
- Gerwert, K., B. Hess, I. Soppa, and D. Oesterhelt. 1989. Role of aspartate 96 in proton translocation by bacteriorhodopsin. *Proc. Natl. Acad. Sci. USA*. 86:4943-4947.
- Gerwert, K., G. Souvignier, and B. Hess. 1990. Simultaneous monitoring of light-induced changes in protein side-group protonation, chromophore isomerization, and backbone motion of bacteriorhodopsin by time-resolved Fourier-transform infrared spectroscopy. *Proc. Natl. Acad. Sci. USA*. 87:9774-9778.
- Harbison, G. S., J. E. Roberts, J. Herzfeld, and R. G. Griffin. 1988. Solid-state NMR detection of proton exchange between the bacteriorhodopsin Schiff base and bulk water. *J. Am. Chem. Soc.* 110:7221-7227.
- Harbison, G. S., S. O. Smith, J. A. Pardo, P. P. J. Mulder, J. Lugtenburg, J. Herzfeld, R. A. Mathies, and R. G. Griffin. 1984a. Solid-state  $^{13}\text{C}$ -NMR studies of retinal in bacteriorhodopsin. *Biochemistry*. 23:2662-2667.
- Harbison, G. S., S. O. Smith, J. A. Pardo, C. Winkel, J. Lugtenburg, J. Herzfeld, R. A. Mathies, and R. G. Griffin. 1984b. Dark-adapted bacteriorhodopsin contains 13-*cis*, 15-*syn* and all-*trans*, 15-*anti* retinal Schiff base. *Proc. Natl. Acad. Sci. USA*. 81:1706-1709.
- Helms, V., and R. C. Wade. 1995. Thermodynamics of water mediating protein-ligand interactions in cytochrome P450cam: a molecular dynamics study. *Biophys. J.* 69:810-824.
- Henderson, R., J. M. Baldwin, T. A. Ceska, F. Zemlin, E. Beckmann, and K. H. Downing. 1990. Model for the structure of bacteriorhodopsin based on high-resolution electron cryomicroscopy. *J. Mol. Biol.* 213:899-929.
- Hermans, J., and S. Shankar. 1986. The free energy of xenon binding to myoglobin from molecular dynamics simulation. *Isr. J. Chem.* 27:225-227.
- Herzfeld, J., S. K. Das Gupta, M. R. Farrar, G. S. Harbison, A. E. McDermott, S. L. Pelletier, D. P. Raleigh, S. O. Smith, C. Winkel, J. Lugtenburg, and R. G. Griffin. 1990. Solid-state  $^{13}\text{C}$  NMR study of tyrosine protonation in dark-adapted bacteriorhodopsin. *Biochemistry*. 29:5567-5574.
- Hildebrandt, P., and M. Stockburger. 1984. Role of water in bacteriorhodopsin's chromophore: resonance Raman study. *Biochemistry*. 23:5539-5548.
- Holz, M., L. A. Drachev, T. Mogi, H. Otto, A. D. Kaulen, M. P. Heyn, V. P. Skulachev, and H. G. Khorana. 1989. Replacement of aspartic acid-96 by asparagine in bacteriorhodopsin slows both the decay of the M intermediate and the associated proton movement. *Proc. Natl. Acad. Sci. USA*. 86:2167-2171.
- Humphrey, W., I. Logunov, K. Schulten, and M. Sheves. 1994. Molecular dynamics study of bacteriorhodopsin and artificial pigments. *Biochemistry*. 33:3668-3678.
- Jorgensen, W. L., J. Chandrasekhar, J. D. Madura, R. W. Impey, and M. L. Klein. 1983. Comparison of simple potential functions for simulating liquid water. *J. Chem. Phys.* 79:926-935.
- Kirkwood, J. G. 1935. Statistical mechanics of fluid mixtures. *J. Chem. Phys.* 3:300-313.
- Kollman, P. 1993. Free energy calculations: applications to chemical and biochemical phenomena. *Chem. Rev.* 93:2395-2417.
- Lewis, A., M. A. Marcus, B. Ehrenberg, and H. Crespi. 1978. Experimental evidence for secondary protein-chromophore interactions at the Schiff base linkage in bacteriorhodopsin: molecular mechanism for proton pumping. *Proc. Natl. Acad. Sci. USA*. 75:4642-4646.
- Mackerell, A. D. Jr., D. Bashford, M. Bellot, R. L. Dunbrack, M. J. Field, S. Fischer, J. Gao, H. Guo, D. Joseph, S. Ha, L. Kuchnir, K. Kuczera, F. T. K. Lau, C. Mattos, S. Michnick, D. T. Nguyen, T. Ngo, B. Prodhom, B. Roux, B. Schlenkerich, J. C. Smith, R. Stote, J. Straub, J. Wierkiewicz-Kuczera, and M. Karplus. 1992. Self-consistent parametrization of biomolecules for molecular modeling and condensed phase simulations. *Biophys. J.* 61:A143.
- Maeda, A., J. Sasaki, Y. Yamasaki, R. Needleman, and J. Lanyi. 1994. Interaction of aspartate-85 with a water molecule and the protonated Schiff base in the L intermediate of bacteriorhodopsin: a Fourier transform infrared spectroscopic study. *Biochemistry*. 33:1713-1717.
- Marti, T., H. Otto, T. Mogi, S. J. Rösselet, M. P. Heyn, and H. G. Khorana. 1991. Bacteriorhodopsin mutants containing single substitutions of serine or threonine residues are all active in proton translocation. *J. Biol. Chem.* 266:6919-6927.
- Meyer, E. 1992. Internal water molecules and H-bonding in biological macromolecules: a review of structural features with functional implications. *Protein Sci.* 1:1543-1562.
- Mogi, T., L. J. Stern, N. R. Hackett, and H. G. Khorana. 1987. Bacteriorhodopsin mutants containing single tyrosine to phenylalanine substitutions are all active in proton translocation. *Proc. Natl. Acad. Sci. USA*. 85:5595-5599.
- Mogi, T., L. J. Stern, T. Marti, B. H. Chao, and H. G. Khorana. 1988. Aspartic acid substitutions affect proton translocation by bacteriorhodopsin. *Proc. Natl. Acad. Sci. USA*. 84:5595-5599.
- Nina, M., B. Roux, and J. C. Smith. 1995. Functional interactions in bacteriorhodopsin: a theoretical analysis of retinal hydrogen bonding. *Biophys. J.* 68:25-39.
- Nina, M., J. C. Smith, and B. Roux. 1993. Ab initio quantum chemical analysis of water-Schiff base interactions in bacteriorhodopsin. *J. Mol. Struct.* 286:231-245.
- Nonella, M., A. Windemuth, and K. Schulten. 1991. Structure of bacteriorhodopsin and in situ isomerization of retinal: a molecular dynamics study. *Photochem. Photobiol.* 54:937-948.

- Oesterhelt, D., and W. Stoekenius. 1971. Rhodopsin-like protein from the purple membrane of *Halobacterium halobium*. *Nature New Biol.* 233: 149–152.
- Oesterhelt, D., and W. Stoekenius. 1973. Functions of a new photoreceptor membrane. *Proc. Natl. Acad. Sci. USA.* 70:2853–2857.
- Onsager, L. 1936. Electric moments of molecules in liquids. *J. Chem. Phys.* 58:1486–1493.
- Otto, H., T. Marti, M. Holz, T. Mogi, M. Lindau, H. G. Khorana, and M. P. Heyn. 1989. Aspartic acid-96 is the internal proton donor in the reprotonation of the Schiff base of bacteriorhodopsin. *Proc. Natl. Acad. Sci. USA.* 86:9228–9232.
- Papadopoulos, G., N. Dencher, G. Zaccai, and G. Büldt. 1990. Water molecules and exchangeable hydrogen ions at the active centre of bacteriorhodopsin localized by neutron diffraction. *J. Mol. Biol.* 214: 15–19.
- Patey, G. N., and J. P. Valleau. 1975. A Monte Carlo method for obtaining the interionic potential of mean force in ionic solution. *J. Chem. Phys.* 63:2334–2339.
- Rothschild, K. J., Y.-W. He, S. Sonar, T. Marti, and H. G. Khorana. 1992. Vibrational spectroscopy of bacteriorhodopsin mutants: evidence that Thr-46 and Thr-89 form part of a transient network of hydrogen bonds. *J. Biol. Chem.* 267:1615–1622.
- Ryckaert, J. P., G. Ciccotti, and H. J. C. Berendsen. 1977. Numerical integration of the Cartesian equation of motions of a system with constraints: molecular dynamics of *n*-alkanes. *J. Comp. Chem.* 23: 327–341.
- Sampogna, R. V., and B. Honig. 1994. Environmental effects on the protonation states of active site residues in bacteriorhodopsin. *Biophys. J.* 66:1341–1352.
- Shi, Y.-Y., A. E. Mark, C. Wang, F. Huang, H. J. C. Berendsen, and W. F. van Gunsteren. 1993. Can the stability of proteins be predicted by free energy calculations? *Protein Eng.* 6:289–295.
- Singh U. C., F. K. Brown, P. A. Bash, and P. A. Kollman. 1987. An approach to the application of free energy perturbation methods using molecular dynamics. *J. Am. Chem. Soc.* 109:1607–1614.
- Smith, S. O., J. Courtin, E. van den Berg, C. Winkel, J. Lugtenburg, J. Herzfeld, and R. G. Griffin. 1989. Solid state  $^{13}\text{C}$  NMR of the retinal chromophore in photointermediates of bacteriorhodopsin: characterization of two forms of M. *Biochemistry.* 28:237–243.
- Song, L., M. A. El-Sayed, and J. K. Lanyi. 1993. Protein catalysis of retinal subpicosecond photoisomerisation in the primary process of bacteriorhodopsin photosynthesis. *Science.* 261:891–894.
- Stern, L. J., and H. G. Khorana. 1989. Structure-function studies on bacteriorhodopsin: individual substitutions of Arg residues by Gln affect chromophore formation, photocycle and proton translocation. *J. Biol. Chem.* 264:14202–14208.
- Subramaniam S., M. Gerstein, D. Oesterhelt, and R. Henderson. 1993. Electron diffraction analysis of structural changes in the photocycle of bacteriorhodopsin. *EMBO J.* 12:1–8.
- Subramaniam, S., T. Marti, and H. G. Khorana. 1990. Protonation state of Asp (Glu 85) regulates the purple-to-blue transition in bacteriorhodopsin mutants Arg 82  $\rightarrow$  Glu: the blue form is inactive in proton translocation. *Proc. Nat. Acad. Sci. USA.* 87:1013–1017.
- Wade, R. C., M. H. Mazar, J. A. McCammon, and F. A. Quiocho. 1990. Hydration of cavities in proteins: a molecular dynamics approach. *J. Am. Chem. Soc.* 112:7057–7059.
- Wade, R. C., M. H. Mazar, J. A. McCammon, and F. A. Quiocho. 1991. A molecular dynamics study of thermodynamic and structural aspects of the hydration of cavities in proteins. *Biopolymers.* 31:919–931.
- Williams, M. A., J. M. Goodfellow, and J. M. Thornton. 1994. Buried waters and internal cavities in monomeric proteins. *Protein Sci.* 3:1224–1235.
- Zaccai, G. 1987. Structure and hydration of purple membranes in different conditions. *J. Mol. Biol.* 194:569–572.
- Zacharias, M., T. P. Straatsma, and J. A. McCammon. 1994. Separation-shifted scaling, a new scaling method for Lennard-Jones interactions in thermodynamic integration. *J. Chem. Phys.* 100:9025–9031.
- Zhou, F., A. Windemuth, and K. Schulten. 1993. Molecular dynamics study of the proton pump cycle of bacteriorhodopsin. *Biochemistry.* 32:2291–2306.